International Journal of Science and Research (IJSR)
ISSN: 2319-7064
SJIF (2019): 7.583

Performance Enhancement of Lead Acid Batteries using Different Surface Areas of Carbon Additives on the Negative Plate

Jagannathan Punjabkesar[1], Heinrich Coetzer[2], Kelvin Nalan Naidoo[3], S. P. Daniel Chowdhury[4]

[1, 2, 3]Auto X (Pty) Ltd (previously Willard Batteries), PE, RSA

[4]Electrical Engineering Department Tshwane University of Technology, Pretoria, RSA

Corresponding Author: *JagannathanP[at]auto-x.co.za, HeineC[at]auto-x.co.za, KelvinN[at]auto-x.co.za, spchowdhury2010[at]gmail.com*

Abstract: ***In a lead acid battery, the negative active material isthe spongy lead and the positive active material isthe lead dioxide. Carbon materials are widely used in the negative active material to improve the lifecycleand alsoto increase the charge acceptance of the battery. Carbon material helpsin reducing the hard sulphation of the negative plate during cycling over a period of time. In this study, negative plates were made with different carbons having different surface areas.The following four readily available carbons were selected for the experiments: a) Graphene with a surface area of 300 m^2/g b) Activated carbon with a high surface area of 1400m^2/g c) Activated carbon with a medium surface area of 800 m^2/g d) Conductive carbon with a surface area of 89 m^2/g e) The negative plates were made with these four types of carbon (0.15%) which were added individually in addition to the existing (0.15%) carbon black (Surface area 40 m^2/g).The results of the carbon combinations on the negative plate were compared with those of the standard negative plates without additional carbon.. A comparison table along with spider plots were made to determine the best carbon combination for African weather conditions.***

Keywords: Negative plate, Active material, Lead acid battery, Carbon additives, Surface area, Dynamic charge acceptance, Life cycle, Water loss, Automotive battery

Glossary and Nomenclature

AGM: Absorptive Glass Mat
BET: Brunauer-Emmett-Teller
CC: Constant Current
CV: Constant Voltage
CCA: Cold Crank Ampere
CHA: Charge
COS: Cast-On-Strap
DOD: Depth-of-Discharge
DCA: Dynamic Charge Acceptance
DCH: Discharge
DCNT: Discrete Carbon Nanotube
DM: De Mineralized
EN : European Norms
EAC: Electrochemically Activated Carbon
EOS: End Of Step
IEC: International Electrotechnical Commission
HER: Hydrogen Evolution Rate
HRPSoC: High Rate Partial State of Charge
MWCNT: Multi Wall Carbon Nanotube
NAM: NegativeActiveMaterial
PAM: PositiveActiveMaterial
PAU: Pause
RPT: Repeat
SEM: Scanning Electron Microscopy
SOC: State Of Charge
SLI: Starting Lighting Ignition
SG: Specific Gravity
SWCNT: Single Wall Carbon Nanotube
LAB: Lead Acid Battery
HRPSOC: High Rate Partial State of Charge.
VRLA: Valve-Regulated Lead Acid.
XRD: X-Ray Diffraction
3BS: Tri Basic Lead sulphate
4BS: Tetra Basic Lead sulphate

1. Introduction

In LAB, both positive and negative active materials were continually upgraded in order to meet the requirements of the current automotive industry.

Recent automotive batteries were used for start stop, micro hybrid in mild hybrid vehicles. In those applications, the lead acid battery must beable to accept the charge faster in order to perform cycling, further, it must be able to operate at HRPSoC conditions and also have less water loss. When lead acid batteries work under these extreme applications, lead sulphate crystals were progressively accumulated over the lead surface, thereby increasing the internal resistance and this leads to battery failure.

In order to avoid progressive accumulation of lead sulphate on the negative plate, different types of carbon were used [1-13]. Carbon materials were able to improve the overall electrical conductivity of the negative plate [11]and to improve the recrystallisation of $PbSO_4$,but this effect depends upon the carbon particle size and concentration of the negative active material [12]. This carbon material also builds a conductive network inside the negative active material [15]. Because of the conductive network, the $PbSO_4$ reduction takes place easily in two different phases:

1) Lead phase
2) Carbon phase

This is known as parallel mechanism of charge [13]which was clearly shown in Figure1.

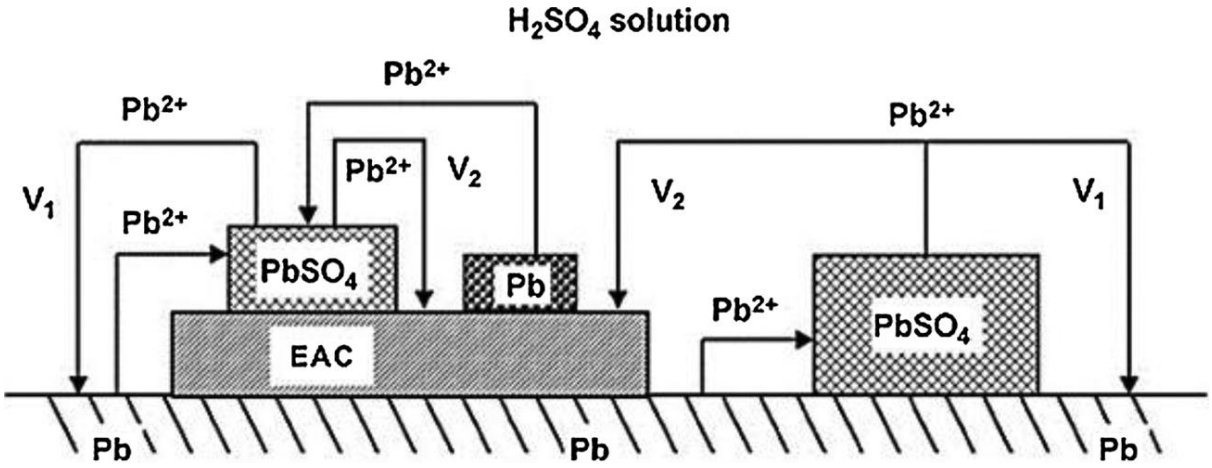

Figure 1: Schematic illustration of Faradaic reaction taking place in negative plates on both lead and carbon surfaces: Courtesy T. Rogachev, P. Nikolov, G. Petkova, et. al [13]

Carbon acts as a capacitor, which stores the charge for a minimal period and then transfers it to the negative active material. By this way the amount of charge can be utilised to a maximum extent [21].

The main disadvantage of carbon is that it has a catalytic effect on the charge reaction. The hydrogen over potentialof the secondary reaction is lower on the carbon/H_2SO_4 interface [6] [16]. Carbon optimization is a key factor for preventing water consumption. New carbon materials such as DCNT, SWCNT, MWCNT were added at a very low concentration for improving the performance [17-20].

This research work is aboutconstant loading of 0.15% of four different surface area carbons in addition to 0.15% standard carbon black (40m^2/g). The plate characterization such as XRD, SEM, BET surface areas were done on the cured and formed plates. The electrical characterizations such as capacity, reserve capacity, CCA, DCA, water consumption and life cycle were also carried out.

2. Experimental Methodology

The experimental methodology consists of preparation of negative plates, positive plates, assembling the battery, charging the battery and analysing the plate. Overall methodology remains the same hence the negative plates were prepared with four different types of carbon as explained in the abstract. The results were analysed and compared with standard negative plate without special carbon.Finally, the best combinationwas selected for battery production.

2.1 Preparation of negative plate

Negative plates were prepared from different carbons with different surface areas and tested for performance enhancement. The carbons selected for the experiments were:

1) Graphene with a surface area of 300 m^2/g
2) Activated carbon with a high surface area of 1400m^2/g
3) Activated carbon with a medium surface area of 800 m^2/g
4) Conductive carbon with a surface area of 89 m^2/g

These four types of carbon (0.15%) were added individually in addition to the existing (0.15%) Carbon black (Surface area 40 m^2/g) and the negative plates were made with all the combination of carbons. The results were compared with the standard negative plate without speciality carbon.

2.1.1 Using Graphene additive

Negative pastewasprepared by addition of 0.15% Graphenewitha surface area of 300 m^2/g along with 0.15 % carbon black, 0.175 % Vanisperse A, 0.2 % poly propylene

fibre, 0.5 % barium sulphate, 11.5 % water. Wet mixing ofthe additive was done for 2 minutes for uniform dispersion. Oxide with a degree of oxidation of 75 % PbO was added to the wet additive mix. After the oxide addition, it was wet mixed for 2 minutes.Sulphuric acid (9.0%, SG 1.4) was added at the rate of 9 kg/min. Once the acid was added and the final mix was done, the density of the paste and moisture content of the paste were checked. Throughout the mixing process, peak temperature was maintained below 58˚C and the dump temperature was maintained below 45˚C. 80g of paste was pasted on the Pb-Ca grid (CAN alloy from RSR) with a surface area of 110mm x 145mm. After pasting this over the surface of the grid, the plate was taken to the curing chamber. Curing/drying schedule is tabulated in Table 1.

Table 1: Curing/Drying

Stage	Temperature(˚C)	Humidity (%)	Hours
Curing	55	100	12
Curing	55	80	6
Drying	70	0	12

Paste morphology analysis and material characterization of the plate, which is listed in Table 2 and Table 3.

Table 2: Paste morphology analysis

Parameter	Graphene 300 m^2/g (0.15%)	Activated Carbon 1400 m^2/g (0.15%)	Activated Carbon 800 m^2/g (0.15%)	Conductive Carbon 89 m^2/g (0.15%)	Standard Negative
Oxide free Lead (%)	25%	25%	25%	25%	25%
Paste Density(g/cc)	4.42	4.41	4.40	4.41	4.40
Moisture (%)	10.2	10.1	10.2	10.1	10.2
Paste free Lead (%)	12.2	11.9	12.0	12.2	12.5
Free Lead after curing(%)	2.9	2.8	2.9	2.7	3.0
After Curing Moisture(%)	0.8	0.9	0.8	0.9	0.8

Procedure for XRD/BET/SEM:
The procedure given below, has been followed throughout the experiment.

XRD: A spatula was used to remove pieces of active materials from the middle and four corners of the formed plates and were ground using a mortar and pestle. The material was pressed into a standard polycarbonate PXRD sample holder. It ensures that a limited preferred orientation was induced onto the sample surface.

BET: A spatula was used to remove pieces of active materials from the middle and four corners of the formed plates. Samples were weighed out (2 – 4g) and inserted into BET sample tubes. These weighed samples were degassed with a constant flow of nitrogen at 90˚C for 2 hours and at 110˚C overnight.

SEM: A spatula was used to remove pieces of active materials from the middle of the formed plates. The samples were placed on a sample holder and gold plated.

Table 3: Material Characterization XRD/BET

Parameter	Graphene 300 m^2/g (0.15%)	Activated Carbon 1400 m^2/g (0.15%)	Activated Carbon 800 m^2/g (0.15%)	Conductive Carbon 89 m^2/g (0.15%)	Standard Negative
Pb(%)	0.01	0.08	0.12	0.11	0.15
3PbO. $PbSO_4.H_2O$	95.23	95.16	94.62	93.57	94.57
A-PbO(%)	4.23	4.50	4.92	4.47	4.98
PbO. $PbSO_4$ (%)	0.41	0.26	0.34	0.76	0.30
Hydrocerusite(%)	0.13	ND	ND	0.11	ND

2.1.2 Using Activated Carbon with surface area of 1400 m^2/g
Negative paste was prepared by the addition of 0.15% activated carbon with a surface area of 1400 m^2/g along with 0.15 % carbon black, 0.175 % Vanisperse A, 0.2 % poly propylene fibre, 0.5 % barium sulphate, and 11.5 % water. Wet mixing ofthe additive was done for 2 minutes for uniform dispersion. Oxide with a degree of oxidation of 75 % PbO was added to the wet additive mix. After the oxide addition, it was wet mixed for 2 minutes.Sulphuric acid (9.0%, SG 1.4) was added at the rate of 9 kg/min. Once the acid was added and the final mix was done, the density of the paste and moisture content of the paste were checked.Throughout the mix, peak temperature was maintained below 58˚C and the dump temperature was maintained below 45˚C.

80g of this paste was pasted on the Pb-Ca grid (CAN alloy from RSR) with a surface area of 110mm x 145mm. After pasting over the surface of the grid, the plate was taken to the curing chamber. Curing/drying schedule is tabulated in Table 1.
Paste morphology analysis and material characterization of the plate, which is listed in Table 2 and Table 3.

2.1.3 Using Activated Carbon with surface area of 800 m^2/g
Negative paste was prepared by the addition of 0.15% activated carbon with a surface area of 800 m^2/g along with 0.15 % carbon black, 0.175 % Vanisperse A, 0.2 % poly propylene fibre, 0.5 % barium sulphate, and 11.5 % water. Wet mixing ofthe additive was done for 2 minutes for uniform dispersion. Oxide with a degree of oxidation of 75 % PbO was added to the wet additive mix. After the oxide addition, it was wet mixed for 2 minutes.Sulphuric acid (9.0%, SG 1.4) was added at the rate of 9 kg/min. Once the acid was added and the final mix was done, the density of the paste and moisture content of the paste were checked.Throughout the mix, peak temperature was maintained below 58˚C and the dump temperature was maintained below 45˚C.

80g of this paste was pasted on the Pb-Ca grid (CAN alloy from RSR) with a surface area of 110mm x 145mm. After pasting over the surface of the grid, the plate was taken to the curing chamber. Curing/drying schedule is tabulated in Table 1.

Paste morphology analysis and material characterization of the plate, which is listed in Table 2 and Table 3.

2.1.4 Use Conductive Carbon with surface area of 89 m^2/g

Negative paste was prepared by the addition of 0.15% conductive carbon with a surface area of 89 m^2/g along with 0.15 % carbon black, 0.175 % Vanisperse A, 0.2 % poly propylene fibre, 0.5 % barium sulphate, and 11.5 % water. Wet mixing ofthe additive was done for 2 minutes for uniform dispersion. Oxide with a degree of oxidation of 75 % PbO was added to the wet additive mix. After the oxide addition, it was wet mixed for 2 minutes.Sulphuric acid (9.0%, SG 1.4) was added at the rate of 9 kg/min. Once the acid was added and the final mix was done, the density of the paste and moisture content of the paste were checked. Throughout the mix, peak temperature was maintained below 58˚C and the dump temperature was maintained below 45˚C.

80g of this paste was pasted on thePb-Ca grid (CAN alloy from RSR) witha surface area of 110mm x 145mm. After pasting over the surface of the grid, the plate was taken to the curing chamber. Curing/drying schedule is tabulated in Table 1.
Paste morphology analysis and material characterization of the plate, which is listed in Table 2 and Table 3.

2.1.5 Standard Negative plate:

Negative paste was prepared by addition of 0.15 % carbon black, 0.175 % Vanisperse A, 0.2 % poly propylene fibre, 0.5 % barium sulphate, and 11.5 % water. Wet mixing ofthe additive was done for 2 minutes for uniform dispersion. Oxide with a degree of oxidation of 75 % PbO was added to the wet additive mix. After the oxide addition, it was wet mixed for 2 minutes.Sulphuric acid (9.0%, SG 1.4) was added at the rate of 9 kg/min. Once the acid was added and the final mix was done, the density of the paste and moisture content of the paste were checked. Throughout the mix, peak temperature was maintained below 58˚C and the dump temperature was maintained below 45˚C.

80g of paste was pasted on the Pb-Ca grid (CAN alloy from RSR) with a surface area of 110mm x 145mm. After pasting over the surface of the grid, the plate was taken to the curing chamber. Curing/drying schedule is tabulated in Table 1.
Paste morphology analysis and material characterization of the plate, which is listed in Table 2 and Table 3.

2.2 Preparation of Positive Plate

2.2.1 Standard Positive Plate:

Positive paste was prepared by addition of 0.5% tetrabasic seeding crystal, 0.3% poly propylene fibre, and 11.5% water. Wet mixing ofthe additive was done for 2 minutes for uniform dispersion. Oxide with a degree of oxidation of 75 % PbO was added to the wet additive mix. After the oxide addition, it was wet mixed for 2 minutes.Sulphuric acid (10.0%, SG 1.4) was added at the rate of 9 kg/min. Once the acid was added and the final mix was done, the density of the paste and the moisture content of the paste were checked.Throughout the mix, peak temperature was maintained below 58˚C and the dump temperature was maintained below 45˚C.

100g of paste was pasted on the Pb-Ca-Sn grid (009 Alloy from RSR) with a surface area of 110mm x 145mm. After pasting over the surface of the grid the plate was taken into the curing chamber. Curing/drying schedule was tabulated in Table 4.

Table 4: Curing/Drying

Stage	Temperature(˚C)	Humidity (%)	Hours
Curing	75	100	12
Curing	55	80	6
Drying	70	0	12

Paste morphology analysis and material characterization of the plate, which is listed in Table 5 and Table 6.

Table 5: Paste morphology analysis

Parameter	Standard Positive plate
Oxide free Lead (%)	24%
Paste Density(g/cc)	4.28
Moisture (%)	11.5
Paste free Lead (%)	19.5
Free Lead after curing (%)	2.4
After Curing Moisture (%)	0.8

Table 6: Material Characterization XRD:

Parameter	Standard Positive plate
B-PbO(%)	4.14
3PbO. $PbSO_4.H_2O$	6.65
4PbO. $PbSO_4$	59.79
A-PbO(%)	29.42
PbO. $PbSO_4$ (%)	ND
Hydrocerusite(%)	ND

XRD graph & SEM image for the six plates

1) Graphene with a surface area of 300 m^2/g
2) Activated carbon with a high surface area of 1400m^2/g
3) Activated carbon with a medium surface area of 800 m^2/g
4) Conductive carbon with a surface area of 89 m^2/g
5) Standard Negative
6) Standard positive

Were shown in Figure 2 and Figure 3 respectively.

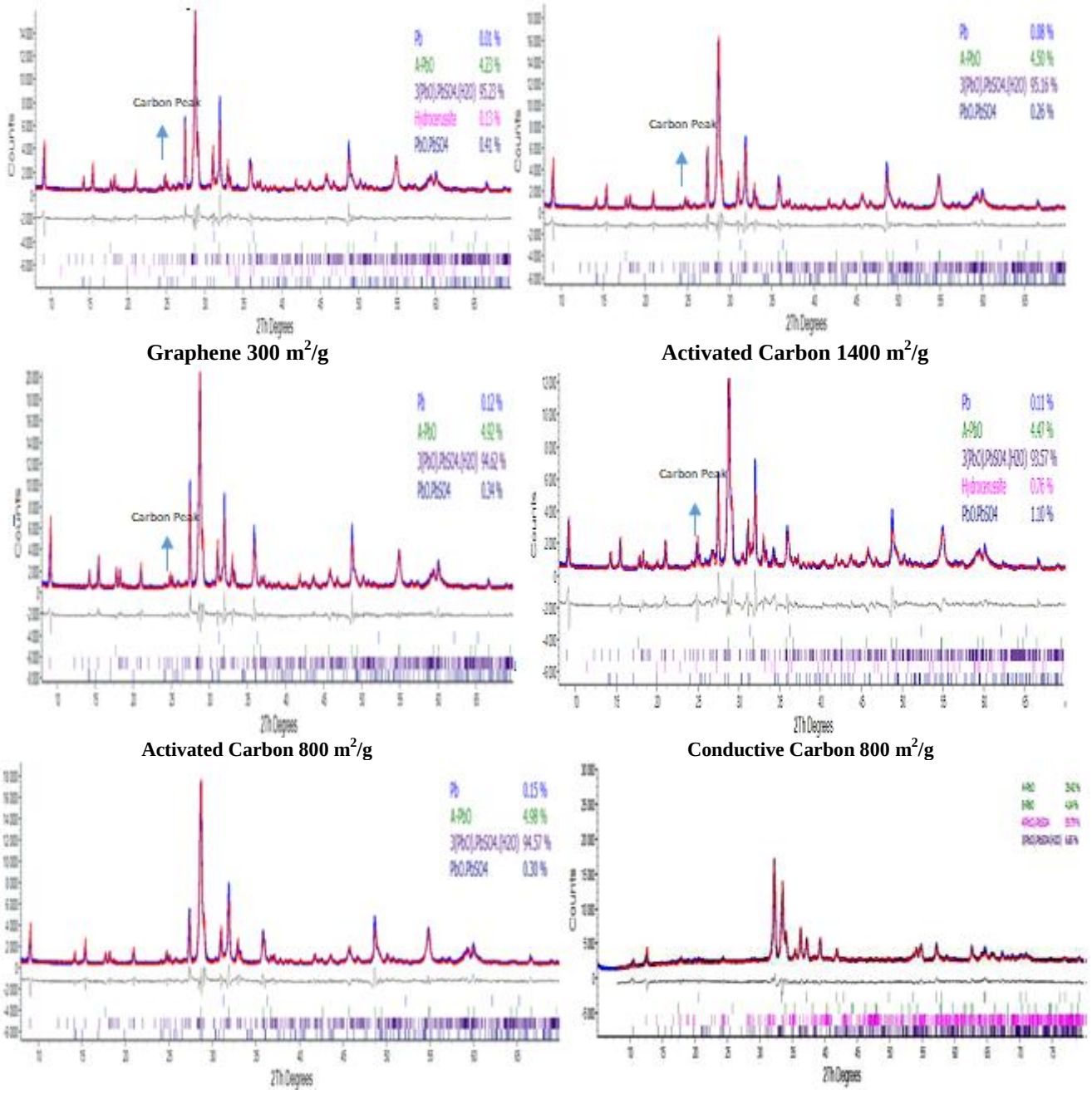

Graphene 300 m^2/g **Activated Carbon 1400 m^2/g**

Activated Carbon 800 m^2/g **Conductive Carbon 800 m^2/g**

Standard Negative **Standard Positive**

Figure 2: XRD pattern for the positive and negative Cured Plate. Carbon Peak around 26.5˚(2θ)

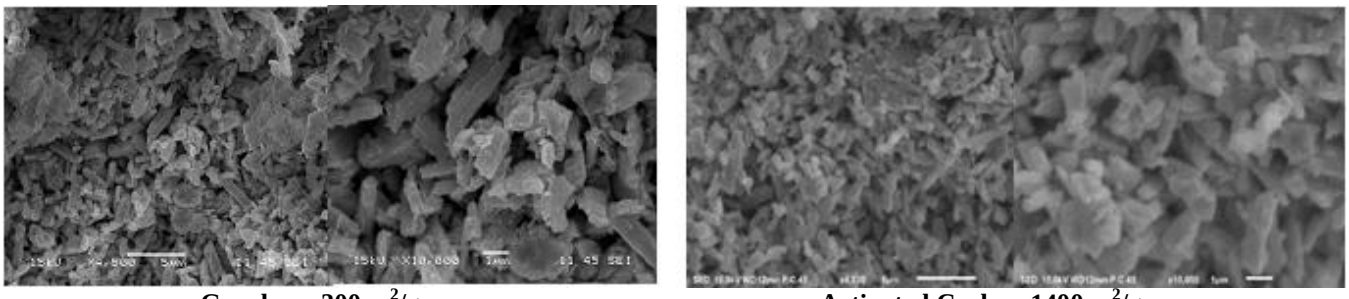

Graphene 300 m^2/g **Activated Carbon 1400 m^2/g**

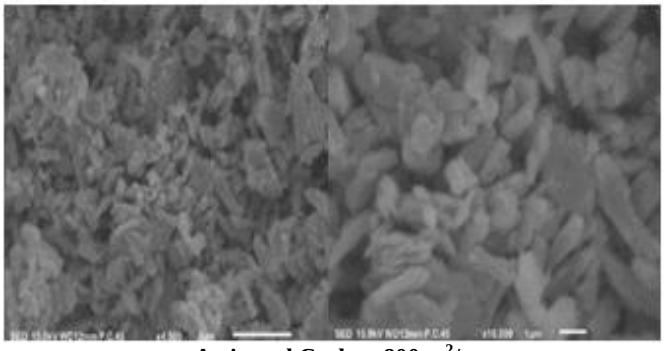

Activated Carbon 800 m^2/g

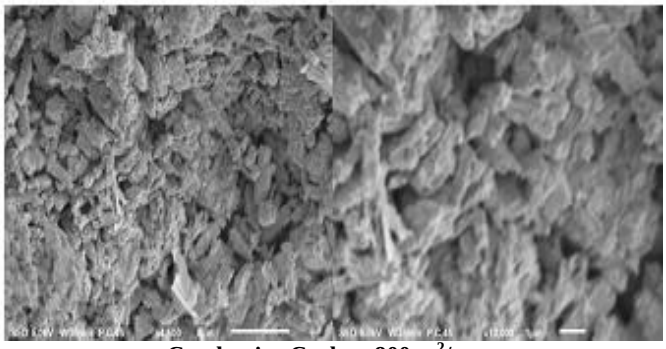

Conductive Carbon 800 m^2/g

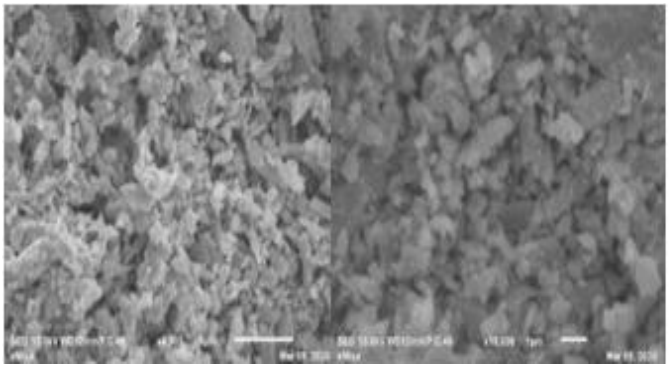

Standard Negative

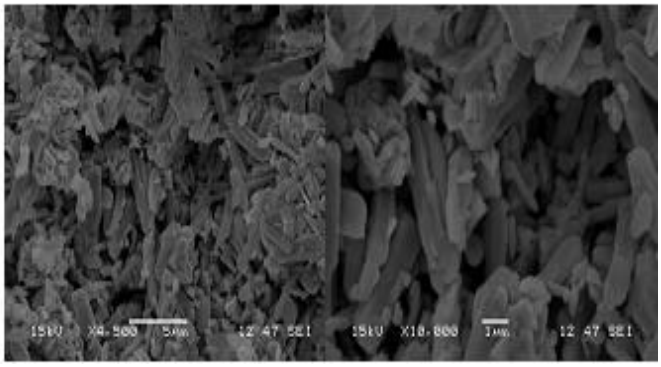

Standard Positive

Figure 3: SEM image for positive and negative plate. Uniform 3BS crystal structure with size of 2 to 3 micron seen on the negative plate and uniform 4BS crystal structure with crystal size of 5 to 7 micron seen on the positive plate.

2.3 Assembly of Battery

L3 Batteries were assembled with 7 positive plates and 8 negative plates in each cell. Batteries were made with the above mentioned carbon negative plate combinations and standard positive plate.

2.4 Charging of Batteries:

All the batteries were filled with electrolyte with a specific gravity of 1.120. The temperature of the acid maintained during filling was below 10˚C. After acid filling the batteries were charged using the profile mentioned in Table 7.

Table 7: Charge profile

Step	Current density (mA/cm^2)	Hours (h)	Input Ah/kg of Dry paste
1	2.5	3	26
2	8.5	4	108
3	0	0.5	0
4	8.5	3	80
5	0	0.5	0
6	8.5	4	108
7	0	0.5	0
8	6.5	5	102
9	0	0.5	0
10	5.5	5	86
Total		26	510

It is clear from the graph shown in Figure4 that higher the surface area of carbon, higher the top of charging voltage during formation.

After charging, the plates were analysed and the batteries were adjusted with operating specific gravity of 1.285 to 1.295 g/cc, and checked for capacity, cold crank, reserve capacity, water consumption, DCA and 17.5% DOD cycling.

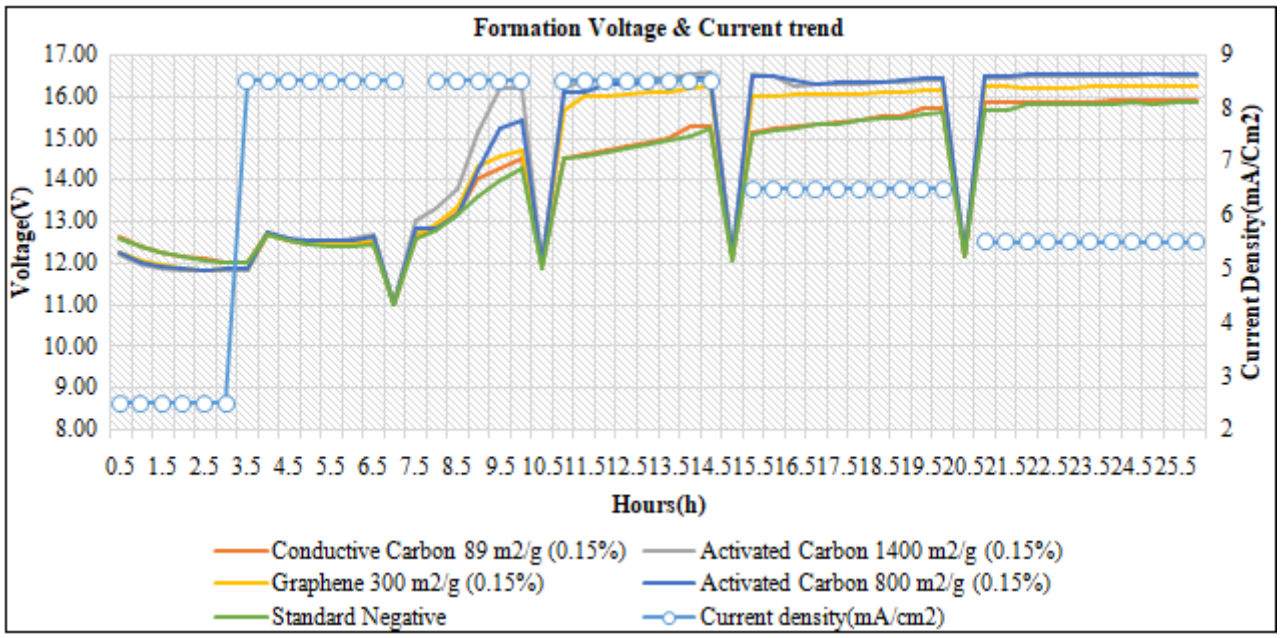

Figure 4: Formation Voltage and current trend graph

2.5 Formed plate Analysis

After formation, the positive plates were washed with DM water until the Ph of the plate reached between 5 to 7.The plateswere dried at 70˚C for 12 hours and were sent forXRD,SEM, BET surface area analysis. The results are tabulated in Table 8.

Negative plates were washed with DM water and dried in a vacuum chamberat 70˚C for 12 hours and were sent forchemical analysis,SEM, BET surface area analysis. The results are tabulated in Table 8. XRD and SEM image of the formed positive plate were shown in Figure 5 and Figure 6.SEM image of the negative plate was shown in Figure 7.

Negative plate/Positive plate characterization:

Table 8: Material Characterization Material Analysis:

Parameter	Graphene 300 m^2/g (0.15%)	Activated Carbon 1400 m^2/g (0.15%)	Activated Carbon 800 m^2/g (0.15%)	Conductive Carbon 89 m^2/g (0.15%)	Standard Negative plate(XRD)	Standard Positive plate(XRD)
Pb(%)	89.6	91.9	91.4	89.2	88.9	NA
$PbSO_4$(%)	5.6	4.1	4.2	5.8	6.0	4.39
PbO(%)	4.8	4.0	4.4	5	5.1	NA
A-PbO_2(%)	NA	NA	NA	NA	NA	24.34
B-PbO_2(%)	NA	NA	NA	NA	NA	71.27
BET SSA(m^2/g)	1.12	2.69	1.87	0.78	0.48	5.82

From Table 8 it is clear that higher the surface area of Carbon, higherthe surface area of plate.

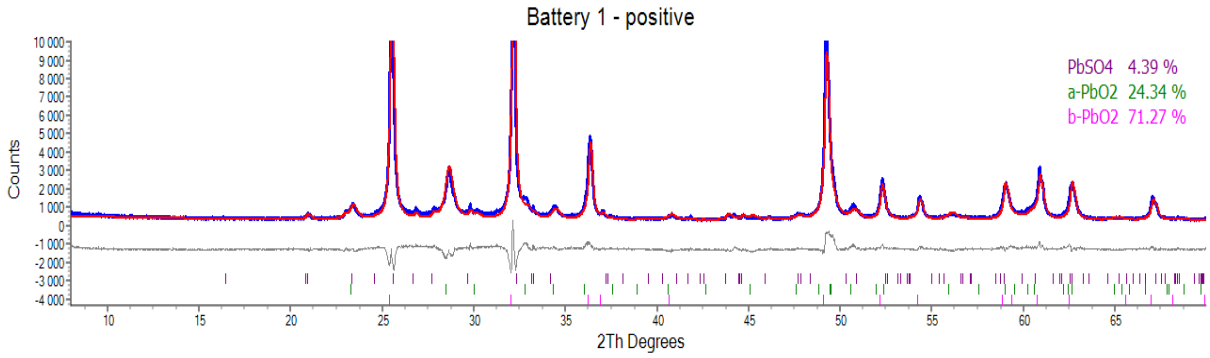

Figure 5: XRD pattern for formed Positive plate

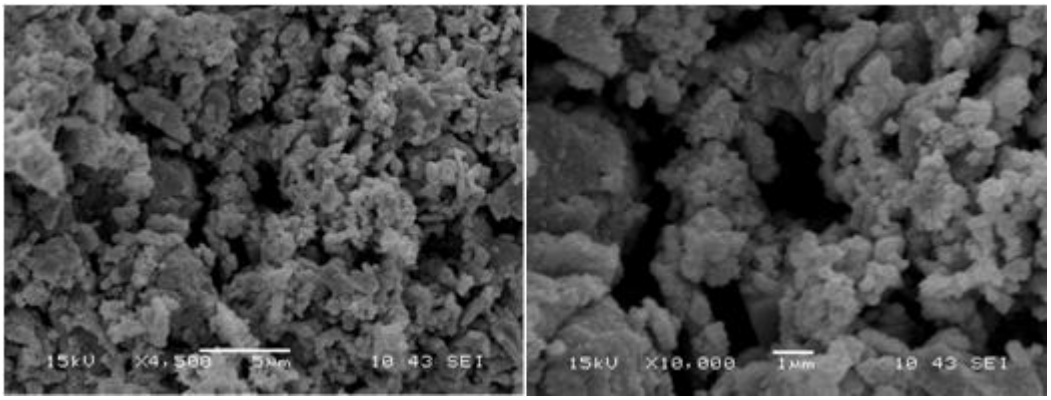

Figure 6: SEM image of formed Positive plate. Small crystal of PbO_2.

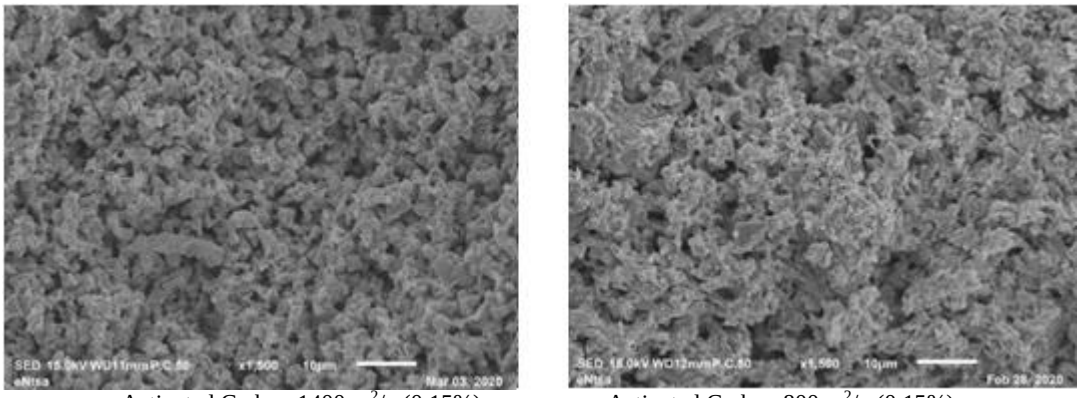

Activated Carbon 1400 m^2/g (0.15%) Activated Carbon 800 m^2/g (0.15%)

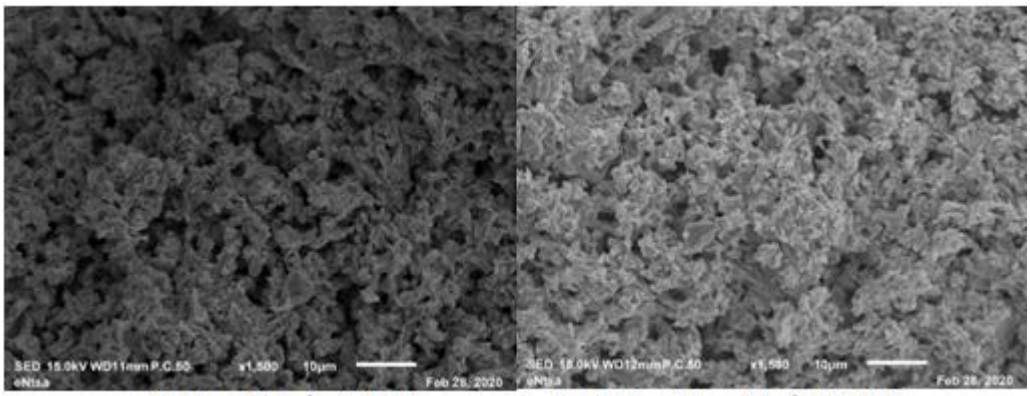

Graphene 300 m^2/g (0.15%) Conductive Carbon 89 m^2/g (0.15%)

Figure 7: SEM image of formed Negative plate.It is clear from the image that higher the surface area of carbon, smaller the size of crystal with more active surfaces.

3. Results & Discussion

Plate characterization:
Negative plateswith different carbon combinationsand the positive plates were analysed for XRD/SEM/BET.

XRD:
Cured negative plate XRD analysis shows mostly 3BS and the graph in Figure 2 shows a slight carbon peak on all the four combinations. On the positive plate,XRDshows mainly 4BS on the cured plate and PbO_2 on the formed plate.

SEM:
The SEM analysisin Figure 3 on cured negative plate shows uniform 3BS crystal with 2 to 3 micron. Positive plate shows uniform 4BS crystal with 5 to 7 micron. Formed plate SEM analysis were shown in Figure 6 and Figure 7. Figure 6 shows the uniform PbO_2 crystal on the positive plate. Figure 7 shows the SEM images of the negative plate with different carbon, from this Figure 7 it is clear that higher the surface area of carbon, finer the crystal with more active surfaces.

BET:
From Table 8 it is quite clear that the BET surface of the negative plate was directly correlated with the surface area of carbon. The following tests were conducted and results were analysed to determine the best performing negative plate.

Electrical testing:
The batteries were tested for 20 hour capacity testing, reserve capacity andcold cranking ability test.
The ratings of the L3 Batterieswere 70Ah/550A(SAE) CCA.

20Hour Capacity testing:
Batteries were discharged at 3.5A till the voltage cut off reached 10.5V.After the test, batteries were recharged for 24 hours with CC and CV charge with current limited to 0.25% C and Voltage limited to 15.9V. The results were tabulated and compared in Table 9 and Figure 8

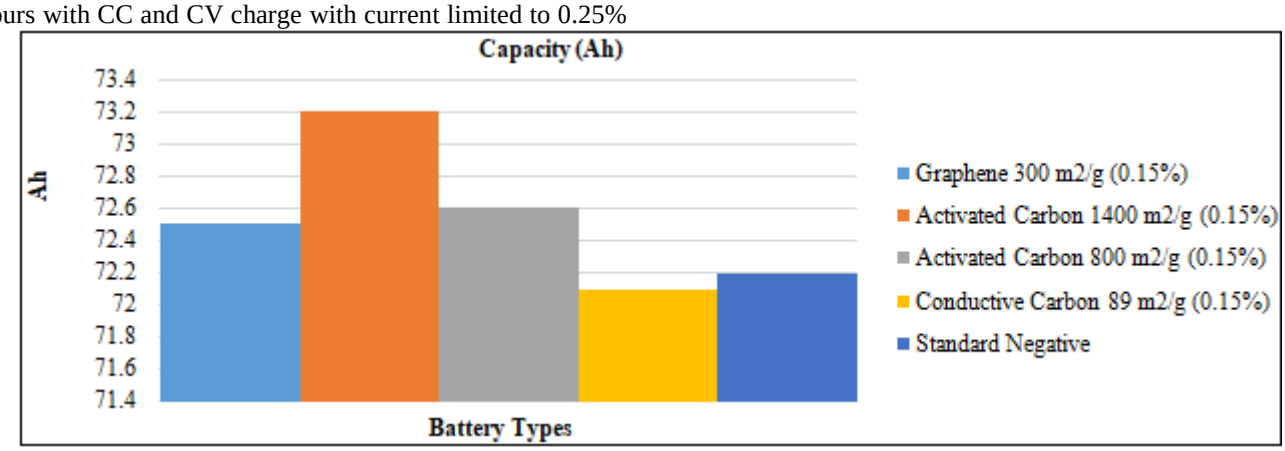

Figure 8: Capacity @ 20 hour rate graph showing no major difference observed on the capacity

Table 9: Basic Electrical testing ,Water consumption, DCA, 17.5% DOD cycling

Parameter	Graphene 300 m^2/g (0.15%)	Activated Carbon 1400 m^2/g (0.15%)	Activated Carbon 800 m^2/g (0.15%)	Conductive Carbon 89 m^2/g (0.15%)	Standard Negative
Capacity(AH)	72.5	73.2	72.6	72.1	72.2
CCA(sec) @ 6V	62.8	62.8	61.6	58.1	57.8
Reserve capacity(AH)	53.4	55.2	54.3	53.2	53.2
Water consumption(g/Ah)	3.2	3.8	3.6	3	2.8
DCA(A/Ah)(I_{DCA})	0.58	0.63	0.61	0.51	0.39
17.5% DOD @ 60˚C cycles	890	950	1052	1240	860

Reserve Capacity testing:
Batteries were discharged at 25A till the voltage cut off reached10.5V.After the test, batteries were recharged for 16 hours with CC and CV charge with current limited to 0.25% C and Voltage limited to 15.9V. The results were tabulated and compared in Table 9 and Figure 9

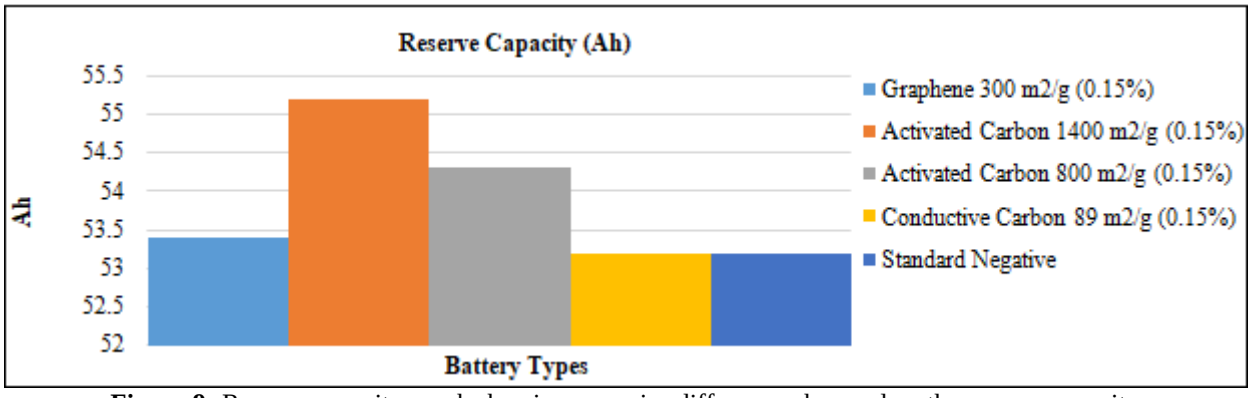

Figure 9: Reserve capacity graph showing no major difference observed on the reserve capacity

Cold Cranking ability:
Batteries were cooled down to -18˚C and discharged at 550A till the voltage cut off reached6V. After the test, batteries were recharged for 16 hours with CC and CV charge with current limited to 0.25% C and Voltage limited to 15.9V. The results were tabulated and compared in Table 9 and Figure 10

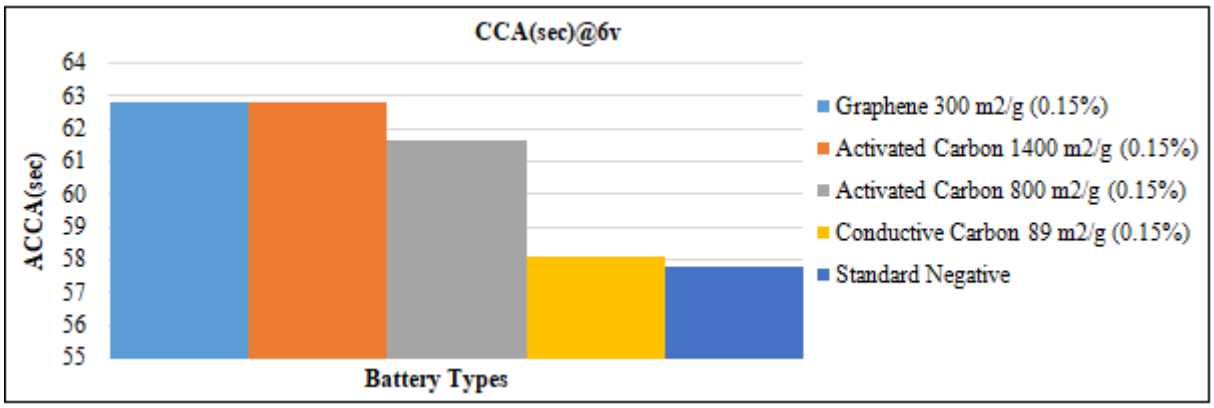

Figure 10: CCA (SAE) graph showing little difference on the cold cranking ability with different carbon

Water Consumption:

During water consumption,the batteries were continuously on charge with constant voltage for 21 days. During this charging process the following reactionstook place on the negative plate.

$$PbSO_4 + H^+ + 2e^- \longrightarrow Pb + HSO_4^- \quad (1)$$
$$Pb + HSO_4^- \longrightarrow PbSO_4 + H^+ + 2e^- \quad (2)$$
$$2H^+ + 2e^- \longrightarrow H_2 \uparrow \quad (3)$$

In the negative plate, lead sulphate is reduced to lead during the charge reaction (1), and lead is oxidized to lead sulphate during the discharge reaction (2). The third possible reaction in the negative plate is related to HER, and this occurs in overcharge conditions or during self-discharge processes.HER is directly linked to float current on the overcharge.hydrogen gassing inside the battery increases with increased float current which leads to high water consumption.This water loss provokes the electrolyte saturation and leads to final battery failure. Water consumption test was conducted on all four different carbonwith different surface areas and the results were tabulated in Table 10

Table 10: Water Consumption data

Parameter	Graphene 300 m^2/g (0.15%)	Activated Carbon 1400 m^2/g (0.15%)	Activated Carbon 800 m^2/g (0.15%)	Conductive Carbon 89 m^2/g (0.15%)	Standard Negative
Water Bath Temperature(˚C)	40	40	40	40	40
Battery Float voltage(V)	14.4	14.4	14.4	14.4	14.4
Battery Float Current after 7 Days(A)	0.65	0.75	0.72	0.62	0.58
Battery Float Current after 14 Days(A)	0.56	0.63	0.6	0.49	0.46
Battery Float Current after 21 Days(A)	0.4	0.48	0.44	0.33	0.29
Water Loss after 21 Days (g/Ah)	3.2	3.8	3.6	3	2.8

Based on the water consumption results in Table 10 it is clear that higher the surface area of carbon, higher the float current which leads to higher water loss.

DCA test:

The DCA Test procedure as Per EN50342-6-2016 is as follows:

Before we start the test batteries must be pre-cycled as shown in Table 11

Table 11: DCA Pre-cycling

Structure	*N°*	*Step*	*t*	*U [V]*	*I [A]*	*Description*	*Data acquisition frequency*	*Result of measurement of each step*
Pre-cycling	10	DCH		> 10,5	25	RC discharge	EOS	RC capacity
	11	CHA	24 h	Uc	5·In	Recharge voltage for flooded / VRLA	EOS	Ah recharged End of charge current
	12	PAU	1 h			Relaxation		
	13	DCH		> 10,5	25	RC discharge	EOS	RC capacity
	14	CHA	24 h	Uc	5·In	Recharge voltage for flooded / VRLA		Ah recharged End of charge current
	15	PAU	1 h			Relaxation		
	16	DCH		> 10,5	1·In	Ce discharge	EOS	Ce Calculate: Crch = Ce – 0,2 · Cn
	17	CHA		Uc	5·In	Recharge voltage for flooded / VRLA		Stop recharge when Crch [Ah] is reached

Table 12: DCA Charge Acceptance qDCA procedure:

Structure	*N°*	*Step*	*t*	*U [V]*	*I [A]*	*Description*	*Data Acquisition frequency*	*Result of measurement of each step*
	20	PAU	min 20 h max 72 h			Rest phase	EOS	OCV
	21	DCApp				DCApp procedure (Table 12)	EOS	Ic = integrated charge 200 s
	22	CHA	12 h	Uc	5·In	Recharge voltage for flooded / VRLA	EOS	
Charge	23	CHA	4 h	18,0 / 14,8	0,5·In /5·In	Recharge voltage for flooded / VRLA	EOS	
Acceptance tests	24	PAU	1 h			Rest phase	EOS	
qDCA	25	DCH	2 h		In		EOS	
	26	PAU	20 h			Rest phase	EOS	
	27	DCApp				DCApp procedure (Table 12)	EOS	Id = integrated charge 200 s
	28	DCH	2 h		In		EOS	
	29	PAU	min 12 h max 72 h			Rest phase	EOS	

Step 23: For flooded batteries, a combination of constant voltage (CV) and constant current (CC) charging (with "unlimited" voltage) is applied. The given voltage limit of 18 V is meant as a safety limit.

Steps 21 and 27: The average charge current of I_c and I_d was calculated.
I_c - The average charge current for 20 pulses after thepreceding charging step 17 (I_c) was calculated from the integrated amount of chargeover all pulses, divided by the total charge time as shown in Table12, step 21
I_d - The average charge current for the 20 pulses after the preceding discharge step 25 (I_d) was calculated from the integrated amount of charge over all pulses, divided by the total charge time as shown in Table12, step 27

Table 13: The DCA_{pp} & DCR_{ss} procedure

DCA_{pp} Part:

Structure	N°	*Step*	*T*	*U [V]*	*I [A]*	*Description*	*Data acquisition frequency*	*Result of measurement of each step*
	30	CHA	10 s	14,8	33,3·In	Charge pulse	EOS	Increment Ic or Id by amount of charge ΔQi
	31	PAU	30 s			Rest phase		
DCApp procedure	32	DCH			20·In	Discharge		Stop discharge when ΔQi [Ah] is reached (x = 1..20)
	33	PAU	30 s			Rest phase		
	34	RPT				Run steps 30 to 33 20 times		

DCR_{ss} part

	N°	*Step*	*T*	*U [V]*	*I [A]*	*Description*	*Data acquisition frequency*	*Result of measurement of each step*
DCRss Cycling Part	40	Connect the resistors						
	41	PAU	12 h			Correct Ah_balance by −0,45 % of Cn	1/h	
	42	DCH	30 s		1·In	Vehicle activation		
	43	DCH	3 s		100	Key engine crank		
	44	CHA	58 s	14,4	33,3·In	Conventional charging		
	45	CAS				Case Ah_balance/Cn of:		
		DCH	30 s		1,25·In	> 0,01		
		CHA	30 s	14,4	33,3·In	< −0,01		
		PAU	30 s			[-0,01..0,01]		
	46	CHA	5 s	15,0	33,3·In	Regenerative charging	1/s	Record amount of charge ΔQ1..19
	47	DCH	9 s		10·In	Engine idle off		
	48	DCH	1 s		100	Engine restart		
	49	CAS				Case Ah_balance/Cn of:		
		DCH	20 s		1,25·In	> 0,01		
		CHA	20 s	14,4	33,3·In	< −0,01		
		PAU	20 s			[-0,01..0,01]		
	50	CHA	5 s	15,0	33,3·In	Regenerative charging	1/s	Record amount of charge ΔQ1..19

	51	CAS				Case Ah_balance/Cn of:		
		DCH	20 s		5·In	> 0		
		CHA	20 s	14,4	33,3·In	< −0,01		
		PAU	20 s			[-0,01..0]		
	52	RPT				Run steps 45 to 51 19 times		
	53	DCH	30 s		2·In			
	54	DCH	120 s		1,05·In			
	55	DCH	330 s		0,4182·In			
	56	PAU	3,33 h			Correct by −0,12 % of Cn Ah_balance	1/h	
	57	RPT				Run steps 42 to 56 3 times		
	58	RPT				Run steps 41 to 57 5 times		
	59	Disconnect the resistors						

I_r -The average regenerative charge current, I_r(data from steps 46 and 50 from Table 13) shall be calculated from the integral amount of charge recharged in all (15V, 5 s) charge pulses, divided by the total charge time.

$$I_{DCA}\left[\frac{A}{Ah}\right] = 0.512\frac{I_c}{C_n} + 0.223\frac{I_d}{C_n} + 0.218\frac{I_r}{C_n} - 0.181$$

Based on the DCA results shown in Table 14 it is clear that higher the surface area of carbon, higher the DCA.

Table 14: DCA Testing Results

Parameter	Graphene 300 m^2/g (0.15%)	Activated Carbon 1400 m^2/g (0.15%)	Activated Carbon 800 m^2/g (0.15%)	Conductive Carbon 89 m^2/g (0.15%)	Standard Negative
I_c(A)	25.92	32.58	30.78	23.24	20.23
I_d(A)	78.48	72.18	75.48	70.48	60.46
I_r(A)	101.76	108.51	104.21	95.55	74.56
I_{DCA}(A/Ah)	0.58	0.63	0.61	0.51	0.39

17.5% DOD cycling testing:

Test Procedure:
DCH- 4*In for 2.5 hrs.
CHG- 7*In for 2400 S
DCH- 7*In for 1800 S
Repeat step 2 and 3 till the voltage drops below 10V.The results were tabulated in Table 9.

Spider plot:

All electrical tests on different surface area of the carbon was compared on the single spider plot which was shown in Figure 11

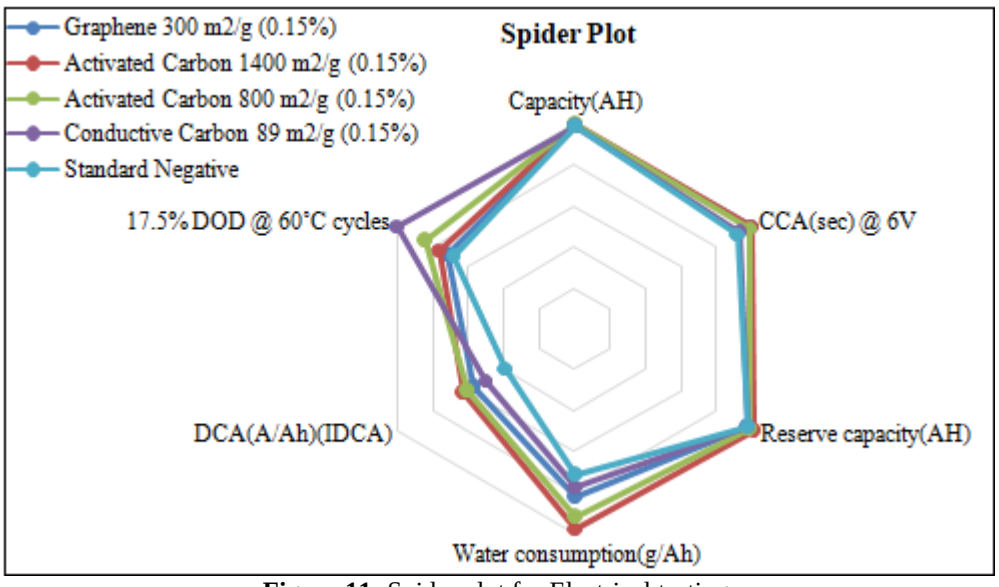

Figure 11: Spider plot for Electrical testing

4. Conclusion

L3 Flooded batteries with different surface area carbons on the negative plate were made using standard processes,materials, and withstandard battery manufacturing equipment. The negative plate'sphysical and chemical changes were monitoredand correlated withits electrical performance. Based on theresults of this study, the following results can be concluded with respect tothe addition of different surface area carbon on the negative plate:

- Physical characterization of the negative plate shows that highersurface area of carbon on the negative plate will lead to higher BET surface area on the negative plate.
- The top of charging voltage on the battery formation was less on the low surface area carbon compared to high surface area carbon.

- Initial capacity, cold crank and reserve capacity were marginally higher on the high surface area carbon.
- The float current during water consumption tests on the high surface area carbon was higher which leads to high water consumption on the batteries.
- Dynamic charge acceptance on the high surface area carbon was excellent because of the higher BET surface area on the negative plate.
- Cyclic performance on the low surface area carbon was high because of less float current & less secondary reaction during the operation.

Based on the above results and spider plot shown in Figure11, it is concluded that conductive carbon with a surface area of 89 m^2/g shows good life @17.5% DOD with less water loss. Even though DCA is reducedwith the conductive carbon,it was better compared to the standard negative plate without speciality carbon. The conductive carbon with a surface area of 89 m^2/g is used in the negative plate in order to enhance the battery life and to improve DCA compared to the standard negative plate, especially in the African climate. The authors were focusing their research to increase the DCA by 1A/Ah, and to increase the cycling to 2500 cycles @17.5% DOD, whilst reducing the water loss to 2 g/Ah. Discrete carbon nanotubes, carbon glass fibre and different carbons were used on both positive and negative active materials..

5. Acknowledgments

The authors would like to acknowledge theTshwane University of Technologyand the Nelson Mandela University for providing necessary research infrastructure and testing facilities to conduct this research study.

6. Funding Information

This was Auto X pty limited company research and development work. No funding from the external agencies.

References

[1] M.Blecua, E.Fatas, P.Ocon, B.Gonzalo, C.Merino, F.de la Fuente, J.Valenciano, F.Trinidad, Graphitized Carbon Nanofibers: new additive for the Negative Active Material of Lead Acid Batteries, ElectrochimicaActa https://doi.org/10.1016/j.electacta.2017.10.067

[2] L. Wang, W. Zhang, L. Gu, Y. Gong, G. Cao, H. Zhao, Y. Yang, H. Zhang, Tracking the morphology evolution of nano-lead electrodeposits on the internal surface of porous carbon and its influence on lead-carbon batteries, Electrochim. Acta. 222 (2016) 376–384. doi:10.1016/j.electacta.2016.10.189.

[3] L. Wang, H. Zhang, G. Cao, W. Zhang, H. Zhao, Y. Yang, Effect of activated carbon surface functional groups on nano-lead electrodeposition and hydrogen evolution and its applications in lead-carbon batteries, Electrochim. Acta. 186 (2015) 654–663. doi:10.1016/j.electacta.2015.11.007.

[4] X. Zou, Z. Kang, D. Shu, Y. Liao, Y. Gong, C. He, J. Hao, Y. Zhong, Effects of carbon additives on the performance of negative electrode of lead-carbon battery, Electrochim. Acta. 151 (2015) 89–98. doi:10.1016/j.electacta.2014.11.027.

[5] J. Valenciano, A. Sánchez, F. Trinidad, A.F. Hollenkamp, Graphite and fiberglass additives for improving high-rate partial-state-of-charge cycle life of valve-regulated lead-acid batteries, J. Power Sources. 158 (2006) 851–863. doi:10.1016/j.jpowsour.2005.11.058.

[6] P. Tong, R. Zhao, R. Zhang, F. Yi, G. Shi, A. Li, H. Chen, Characterization of lead (II)-containing activated carbon and its excellent performance of extending lead-acid battery cycle life for high-rate partial-state-of-charge operation, J. Power Sources. 286 (2015) 91–102. doi:10.1016/j.jpowsour.2015.03.150.

[7] M. Calábek, K. Micka, P. Křivák, P. Bača, Significance of carbon additive in negative lead-acid battery electrodes, 2006. doi:10.1016/j.jpowsour.2005.11.022.

[8] E. Ebner, D. Burow, J. Panke, A. Börger, A. Feldhoff, P. Atanassova, J. Valenciano, M. Wark, E. Rühl, Carbon blacks for lead-acid batteries in micro-hybrid applications – Studied by transmission electron microscopy and Raman spectroscopy, J. Power Sources. 222 (2013) 554–560. doi:10.1016/j.jpowsour.2012.08.089.

[9] M. Fernández, J. Valenciano, F. Trinidad, N. Muñoz, The use of activated carbon and graphite for the development of lead-acid batteries for hybrid vehicle applications, J. Power Sources. 195 (2010). doi:10.1016/j.jpowsour.2009.12.131.

[10] L.T. Lam, R.H. Newnham, H. Ozgun, F.A. Fleming, Advanced design of valve-regulated lead-acid battery for hybrid electric vehicles, J. Power Sources. 88 (2000). doi:10.1016/S0378-7753(99)00515-7.

[11] P.T. Moseley, R.F. Nelson, A.F. Hollenkamp, The role of carbon in valve-regulated lead–acid battery technology, J. Power Sources. 157 (2006) 3–10. doi:10.1016/j.jpowsour.2006.02.031.

[12] D. Pavlov, P. Nikolov, T. Rogachev, Influence of carbons on the structure of the negative active material of lead-acid batteries and on battery performance, J. Power Sources. 196 (2011) 5155–5167. doi:10.1016/j.jpowsour.2011.02.014.

[13] T. Rogachev, P. Nikolov, G. Petkova, Mechanism of action of electrochemically active carbons on the processes that take place at the negative plates of lead-acid batteries, J. Power Sources. 191 (2009) 58–75. doi:10.1016/j.jpowsour.2008.11.056.

[14] M. Blecua, E. Fatas, P. Ocon, J. Valenciano, F. de la Fuente, F. Trinidad, Influences of carbon materials and lignosulfonates in the negative active material of lead-acid batteries for microhybrid vehicles, J. Energy Storage. 11 (2017) 55–doi:10.1016/j.est.2017.01.005.

[15] M. Saravanan, M. Ganesan, S. Ambalavanan, An in situ generated carbon as integrated conductive additive for hierarchical negative plate of lead-acid battery, J. Power Sources. 251 (2014) 20–29. doi:10.1016/j.jpowsour.2013.10.143.

[16] D. Pavlov, T. Rogachev, P. Nikolov, G. Petkova, Mechanism of action of electrochemically active carbons on the processes that take place at the negative

plates of lead-acid batteries, J. Power Sources. 191 (2009) 58–75. doi:10.1016/j.jpowsour.2008.11.056.

[17] S. Logeshkumar, R. Manoharan, Influence of some nanostructured materials additives on the performance of lead acid battery negative electrodes, Electrochim. Acta. 144 (2014) 147–153. doi:10.1016/j.electacta.2014.08.080.

[18] S.W. Swogger, P. Everill, D.P. Dubey, N. Sugumaran, Discrete carbon nanotubes increase lead acid battery charge acceptance and performance, J. Power Sources. (2014) 55–63. doi:10.1016/j.jpowsour.2014.03.049.

[19] N. Sugumaran, P. Everill, S.W. Swogger, D.P. Dubey, Lead acid battery performance and cycle life increased through addition of discrete carbon nanotubes to both electrodes, J. Power Sources. 279 (2015) 281–293.doi:10.1016/j.jpowsour.2014.12.117

[20] R. Marom, B. Ziv, A. Banerjee, B. Cahana, S. Luski, D. Aurbach, Enhanced performance of starter lighting ignition type lead-acid batteries with carbon nanotubes as an additive to the active mass, J. Power Sources. 296 (2015) 78–85. doi:10.1016/j.jpowsour.2015.07.00

[21] Patrick T. Moseley, David A.J. Rand, Alistair Davidson, BorisMonahovUnderstanding the functions of carbon in the negative active-mass of thelead–acid battery: A review of progress ,Journal of Energy StorageVolume 19, October 2018, Pages 272-290